Sensors and Actuators B 193 (2014) 121–127

Contents lists available at ScienceDirect

Sensors and Actuators B: Chemical

journal homepage: www.elsevier.com/locate/snb

Optical properties and sensor applications of bimetallic nanostructures of porphyrins

Mariana Hamer[a], Juan Pablo Tomba[b,1], Irene Noemí Rezzano[a,*,1]

[a] IQUIFIB, National Research Council (CONICET), Faculty of Pharmacy and Biochemistry University of Buenos Aires, Junín 956, CP 1113 Buenos Aires, Argentina

[b] Institute of Materials Science and Technology (INTEMA), National Research Council (CONICET), National University of Mar Del Plata, Juan B. Justo 4302, 7600 Mar del Plata, Argentina

ARTICLE INFO

Article history:
Received 21 September 2013
Received in revised form
21 November 2013
Accepted 23 November 2013
Available online 1 December 2013

Keywords:
Nanostructures
Bimetallic porphyrins
Raman
Sensor

ABSTRACT

The cationic Cu(II) and Fe(III) complexes of tetra(4-pyridyl)porphyrin $[T_4PyP]^{4+}$ have been combined with the anionic $[H_4TPPS]^{2-}$ to obtain bimetallic J-aggregate nanostructures defined by the tendency to form the $Fe^{III}OCu^{II}$ bridge along with electrostatic interactions.

The Resonant Raman spectra of the bimetallic structures revealed subtle but detectable changes of two significant bands: 661 cm^{-1} (attributed to the out-of-plane bending of the Cu—N bond) and 805 cm^{-1} (sensitive to the nature of the axial ligand opposite to the oxo ligand), both indicating the important role of the metallic centers in the formation of the CuFe nanorod aggregate.

The sensing performance of the aggregates was explored monitoring the absorbance changes in the visible region induced by adding different analytes (H_2O_2, NO_2^-, SO_3^{2-} and N_3^-).

The bimetallic nanostructures maintain the J-aggregation structure after successive addition of H_2O_2 with an increasing absorption response at 435 cm^{-1} (monomer band); this architecture was the most sensitive arrangement confirming the synergic effect of the two metals.

1. Introduction

The synthesis of supramolecular assemblies of π-conjugated chromophores has been the subject of intense research over the last years with the aim of obtaining functional and versatile materials to develop innovative photonic and electronic applications, such as solar cells, optical sensors, catalyst, etc. [1]. The physicochemical properties of these materials depend on the interplay of multiple molecular interactions. In fact, they are not only related to the chemical structure of the components but also to the resulting supramolecular architecture and the geometric complementarity [2].

Porphyrins and metalloporphyrins are very well known π-conjugated chromophores with unique optical properties, which show strong tendency to accommodate in face-to-face (H-aggregates) or edge-to-edge (J-aggregates) stacking [3], forming two-dimensional dye crystals and having differential absorption and emission properties [4].

A large number of porphyrins have been incorporated into discrete self-assembled nanostructures with defined shapes and sizes through π–π stacking, hydrogen-bonding, metal-mediated complexation and electrostatic forces [5]. Recently, Shelnutt' group described a new type of hollow nanotubes formed by ionic self-assembly of two porphyrins with opposite charge that show tunable optical properties related to the type of porphyrin cores [6]. They reported that the formation of nanotubes is highly dependent on the coordination geometry of the ionic porphyrins [7], because no nanotubes were formed when a metal free porphyrin or a metal with flat square coordination (e.g., Cu^{II}) were used.

The porphyrinic nanotubes are especially interesting because they are suitable for sensing applications. It has been described that certain organic compounds can be included in the inner cavity of the nanotubes, altering the supramolecular arrangement and the optical signature [8].

In our experience with bimetallic structures of porphyrins, we observed a significant enhancement of the optical and electrochemical response to certain analytes (H_2O_2, N_3^-, SO_3^-, NO_2^-) when Cu(II) and Fe(III) complexes of porphyrins were combined. These results were observed regardless the type of substituents in the aromatic ring [9,10] and attributed to the linear accommodation of the metallic centers through an oxo ligand bound of the type μ-oxo-heme-copper complex [11]. This idea was reinforced by the fact that the increased signal can only be observed in the presence of oxygen.

* Corresponding author. Tel.: +54 1149648262; fax: +54 1138319710.
E-mail address: irezzano@ffyb.uba.ar (I.N. Rezzano).
[1] CONICET permanent staff.

0925-4005/$ – see front matter © 2013 Elsevier B.V. All rights reserved.
http://dx.doi.org/10.1016/j.snb.2013.11.077

Here, we describe new bimetallic nanostructures of porphyrins with particular optical properties highly dependent on the molecular organization. The novelty of this design resides in the incorporation of oxo-bridged Fe and Cu cationic porphyrins in an ionic self-assembly of functional materials. The resulting molecular arrangements are explored as a new material for sensing different analytes.

2. Experimental

2.1. Reagents

5,10,15,20-Tetrakis-(4-sulfonatophenyl)-porphyrin (hereafter $[H_4TPPS]^{2-}$) and 5,10,15,20-tetrakis-(4-pyridyl)-porphyrin ($[TPyP]^{4+}$) were purchased from Sigma–Aldrich and used without further purification. Fe(III) and Cu(II) complexes of 5,10,15,20-Tetra(4-pyridyl)-21H,23H-porphine ($[Fe\text{-}TPyP]^{5+}$ and $[Cu\text{-}TPyP]^{4+}$) were prepared according to standard procedure [12]. All other reagents were obtained from Merck and Fluka. Water was deionized and filtered using a Millipore water purification system (18 MΩ).

2.2. Apparatus

A HP8452 diode array spectrophotometer and a quartz crystal cell were used to obtain the UV spectra.

Nanorods size was verified by TEM. Porphyrin nanorods in aqueous dispersion were imaged in a Phillips CM200 Transmission Electron Microscope after placing drops of dispersion onto gold grids, formwar of 400 mesh (SPI, PA, USA), and leaving the liquid to dry in air at room temperature. The scanning electron micrographs were obtained using a Zeiss DSM982 GEMINI SEM with Field Emission Gun (FEG), operated at 3 kV.

Raman scattering spectra were collected on a Renishaw in-Via Reflex confocal microspectrometer, equipped with a CCD detector of 1024 × 256 pixels, an holographic grating of 2400 groves/mm and a 50-mW Ar laser (514 nm wavelength) as excitation source. Spectra were measured in the 100–1600 cm^{-1} Raman shift region, at 1 cm^{-1} spectral resolution. Measurements were carried out in conditions of *high confocality* (3 pixels of the CCD detector and 20 μm slit width) through a 100× Leica metallurgical objective (numerical aperture of 0.9), which limits the diameter of the laser beam to about 1 μm.

2.3. Nanorods synthesis

Porphyrin nanorods were prepared following the procedure described by Shelnutt and co-workers [7], mixing aqueous solutions of the two porphyrins. The mixture was left in the dark at room temperature for 72 h. All the solutions containing the porphyrin nanorods were stored in the dark at room temperature.

The amount of porphyrin effectively incorporated to the nanotubes structures was calculated by quantifying the amounts of

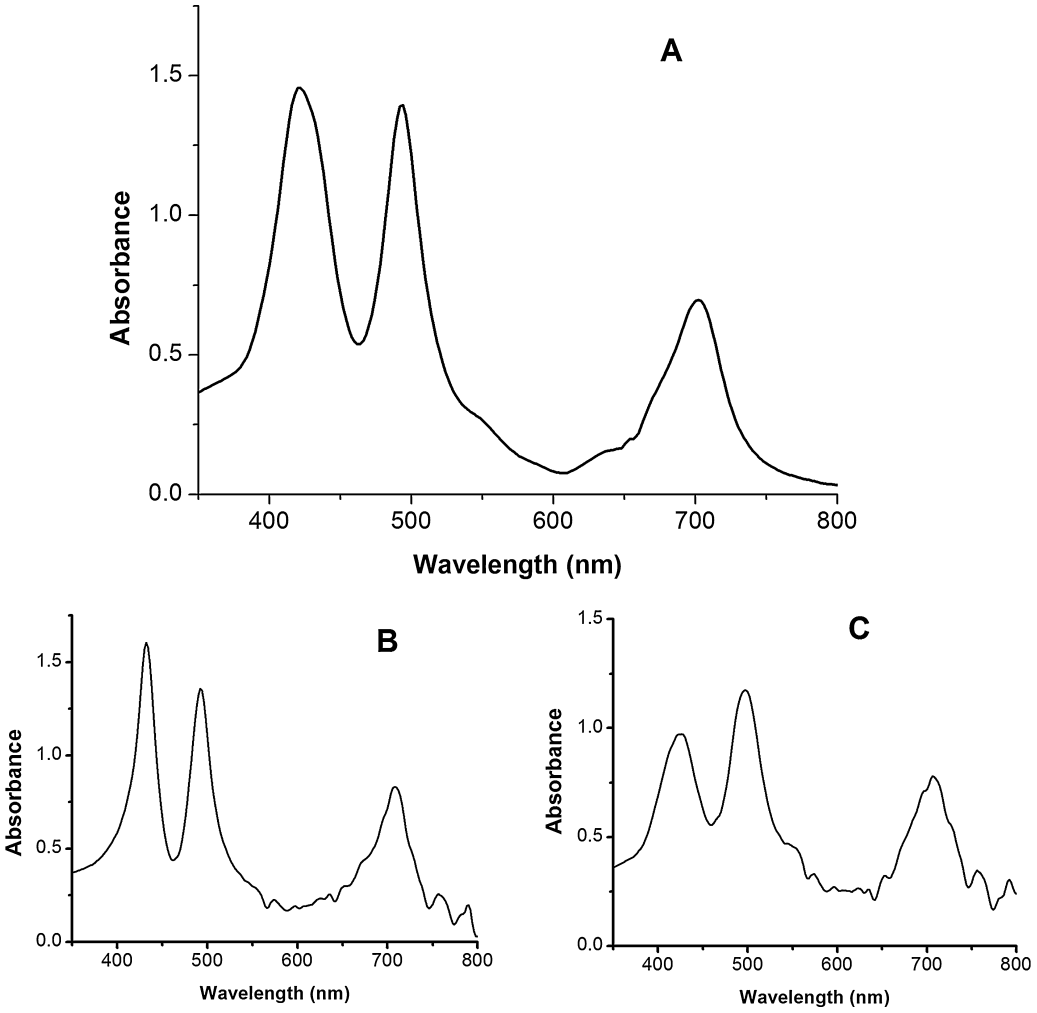

Fig. 1. Absorbance spectra of: (A) FeCuNR, (B) FeNR and (C) CuNR in 0.1 mol/L aqueous HCl solution.

each of the porphyrines removed from the solution. The remaining porphyrin concentrations were calculated from the extinction coefficients of diluted stock solutions of the porphyrin monomers. This experiment revealed that the ratio of the different porphyrins in the nanotubes is 2:2:9 corresponding to $[Fe\text{-}TPyP]^{5+}$:$[Cu\text{-}TPyP]^{4+}$:$[H_4TPPS]^{2-}$.

The absorption spectra were obtained adding different aliquots of H_2O_2 (20 mM), $NaNO_2$ (105 mM), NaN_3 (50 mM) and Na_2SO_3 (80 mM). All these measurements were performed at pH 2.0 to maintain the porphyrin nanostructures.

3. Results and discussion

3.1. Characterization

The cationic Cu(II) and Fe(III) complexes ($[Cu\text{-}TPyP]^{4+}$ and $[Fe\text{-}TPyP]^{5+}$) have been combined with the anionic $[H_4TPPS]^{2-}$ to obtain bimetallic nanostructures. The measured UV-vis spectrum of the acid solutions (Fig. 1) has absorption maxima in the "monomer" Soret region (435 nm) [13], as well as intense bands at 492 nm and 710 nm, which are the signature that indicates formation of J-aggregates [14] in every system.

Transmission electron microscope (TEM) images of the porphyrin aggregates (Fig. 2) reveal the formation of hollow structures

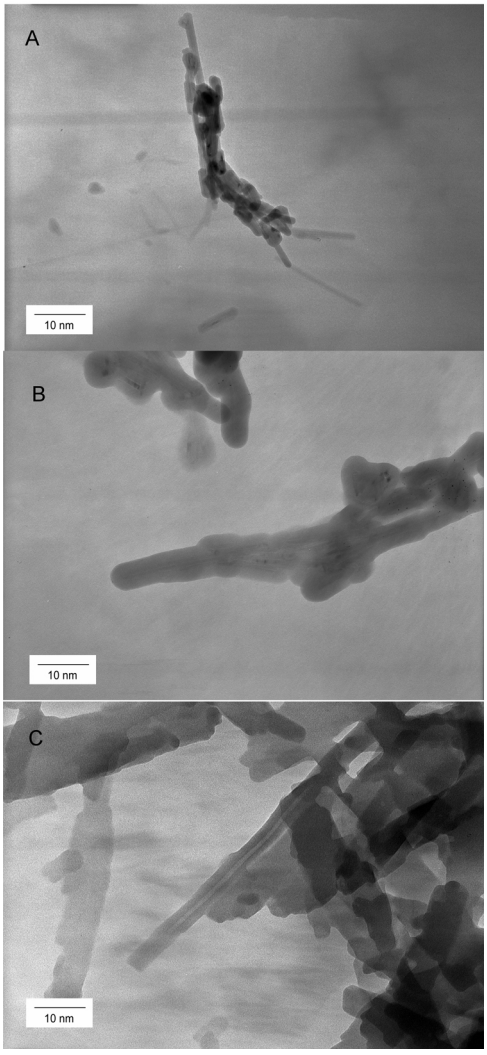

Fig. 2. TEM images (magnification 100×): (A) CuNR, (B) FeNR and (C) FeCuNR.

Table 1
Raman frequencies (in cm^{-1}) of the nanostructures. Excitation wavelength: 514 nm.

Fe NR	Cu NR	FeCu NR	Assignment
382	385	380	Metallation of TPyP
417	419	418	Metal-ligand signals
443			Fe(III)-OH
452	453	455	Metal-ligand signals
498	493	493	Metal-ligand signals
548	546	546	Metal-ligand signals
620	620	619	Metallation of TPyP
	661		Cu—N bond
805			Fe(IV)=O
	855	855	δ-sym py
1002			δ-py breath
1159	1159	1161	δ-asym C_β-H
1194	1192	1192	δ-asym C_α-C_β
1340	1337		Metallation of TPyP

NR, nanorod; TPyP, meso-tetra (4 pyridyl) porphine; Py, pyridine.

of CuNR (Fig. 2A), FeNR (Fig. 2B) and FeCuNR (Fig. 2C) (NR, nanorod). They show different shapes, but are mostly rodlike with lengths in the range 50–70 nm; the inner channel can be clearly observed. In the case of bimetallic aggregates (Fig. 2C), the tubes appear more collapsed. Scanning electron microscope (SEM) images (not shown) revealed morphology of flattened nanorods [15].

The mid-frequency (650–2000 cm^{-1}) diffuse-FTIR spectra of the nanorods showed no significant differences in terms of metal characterization (not shown). On the contrary, the Raman spectrum proved to be a very useful tool to elucidate the internal organization of the porphyrins in the aggregates. The Resonance Raman spectra were acquired with a laser line of 514 nm, in resonance with the J-aggregate absorption band [16], which enhances the characteristic Raman modes of these nanostructures [3,7]. Raman peaks were assigned in the context of earlier work on monometallic agregates [16–21]. Fig. 3 shows bands at 1592, 1563, 1561, 1475 and 1427 cm^{-1}, also found in the widely studied $[H_4TPPS]^{2-}$ self-aggregates [16,17]. Resonant Raman (RR) spectra present vibrational modes particularly sensitive to the ring deformation in the low frequency region (below 850 cm^{-1}); they differ depending on whether the porphyrin ring is planar or domed. The bands at 620, 550 and 498 cm^{-1} have been attributed to vibrations involving the porphyrin metal chelation [18] and, in this case, indicate the presence ($[Cu\text{-}TPyP]^{4+}$ and $[Fe\text{-}TPyP]^{5+}$) included in the nanostructure. This region also contains the metallic complex marker υ_8 (~385 cm^{-1}) attributed to metal coordination (Me–N stretching mode) and methine bridge bending $C_\alpha C_m C_\alpha$ [22] band. This vibrational mode is clearly observed for all the nanostructures reported in Table 1 and confirms the presence of $[Cu\text{-}TPyP]^{4+}$ and $[Fe\text{-}TPyP]^{5+}$.

In order to understand the geometric organization of the aggregates, we focused our attention in two bands (805 cm^{-1} and 661 cm^{-1}) which are present in the monometallic structures and absent in the bimetallic nanorods (Table 1). The band at 805 cm^{-1} is only observed in the oxidized form $O{=}Fe^{IV}$ of the monometallic FeNR, which is most likely formed in the presence of oxygen at acidic pHs. This band has been described as highly sensitive to the nature of the axial ligands in trans position to the iron-oxo moiety [23]. Similarly, the monometallic aggregate CuNR exhibits the corresponding band at 661 cm^{-1}, which was attributed to the out-of-plane bending of the Cu—N bond [19] and considered a peak marker of the presence of copper complexes of porphyrins [20]. The intensity of these two bands significantly diminished in the RR spectra of the bimetallic nanostructure, indicating a change in the coordination sphere of both metals and suggesting a more rigid conformation in comparison with the monometallic aggregates. In accordance

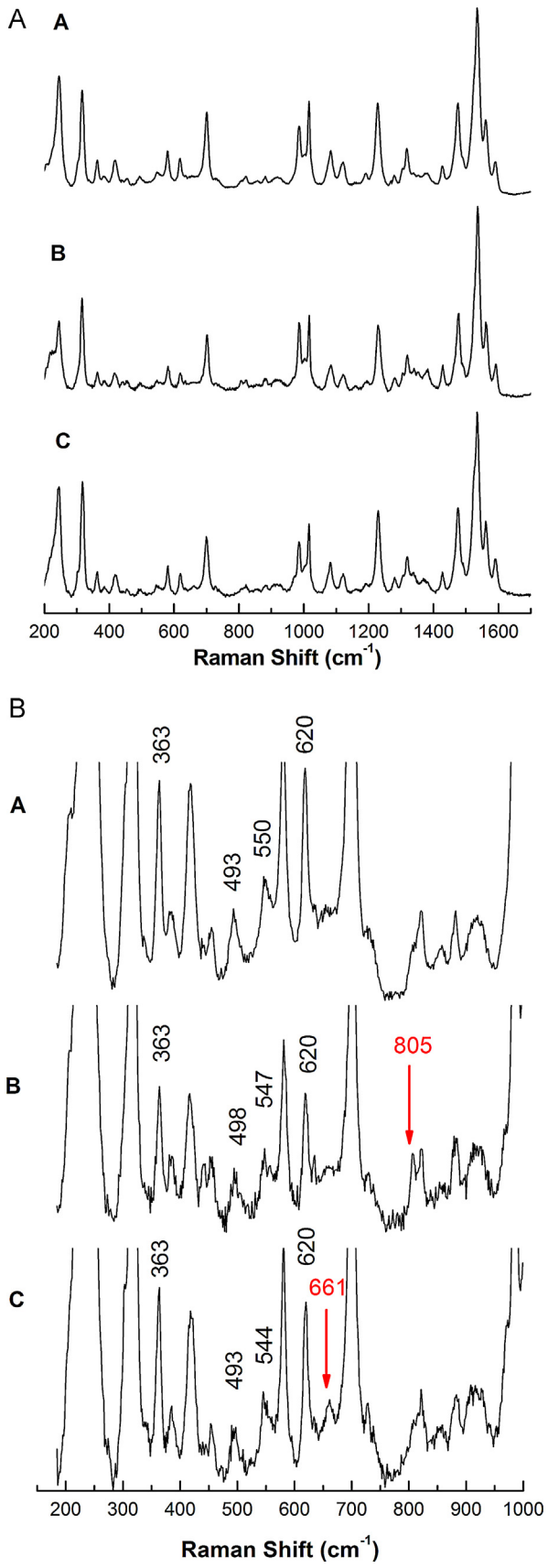

Fig. 3. Resonance Raman spectra of (A) FeCuNR, (B) FeNR and (C) CuNR, complete spectrum and highlighted spectrum between 200 and 1000 cm^{-1}. Excitation wavelength: 514 nm.

to the spectroscopic and microscopic results described, that reinforce the idea of the metallic centers linked through a bridge $Fe^{III}OCu^{II}$, we propose two different arrays depicted in Scheme 1.

3.2. Optical response

To evaluate the effectiveness of the nanorods as sensing materials, we measured the absorbance changes induced by different analytes which are able to coordinate the metalloporphyrins. In all cases, absorbance spectra of the monomers showed negligible changes (not shown), while the aggregates suffered significant modifications of the optical response. These changes resulted more noticeable for the bimetallic structures. Fig. 4 shows the resulting absorption spectra of CuFeNR solutions after successive additions of H_2O_2 (A), $NaNO_2$ (B) Na_2SO_3 (C) and NaN_3 (D) which have been widely described as axial ligand of metalloporphyrins [24–27]. Taking into account the stability of these compounds at pH 2, we can say that the actual analytes measured were H_2O_2, SO_2 and HN_3. The nitrous acid, formed from anion NO_2^- at pH 2, disproportionate to nitric oxide and nitric acid [28].

$$3HNO_2 \rightarrow HNO_3 + 2NO + H_2O$$

Fig. 4(A–D) reveals the proportional increase of the peak at 435 nm with analyte concentration. An interesting point is that the H_2O_2 and HN_3 (Fig. 4A and D) show analogous spectra, suggesting similar coordination structure.

The reductive nitrosylation of the $[Fe^{III}TMPyP]^{5+}$ in the presence of NO(g) to $[Fe^{II}(NO)TMPyP]^{4+}$ at different pH values, has been reported [29]. The reaction is accompanied by a blue shift characteristic of nitric oxide binding to iron(II) porphyrins. With these ideas in mind, we attributed the incipient shoulder ~400 nm (Fig. 4B and C) to the reduced forms of the metallic centers formed in the presence of NO or SO_2.

To compare the sensing behavior of the bimetallic nanorod with the monometallic structures we studied the visible spectra of the aggregates in the presence of H_2O_2. This analyte was chosen because it showed the most stable and reproducible response. Fig. 5 shows the UV–vis spectra of the nanorods at different concentrations of H_2O_2 (10–100 μM). Fig. 5A, corresponding to the monometallic FeNR, depicts a diminution of bands at 490 nm and 710 nm along with a slight increase of the monomer band (435 nm) that would indicate disaggregation of the NR or partial the oxidative destruction of the aromatic ring. Conversely, the monometallic CuNR keeps unchanged under similar experimental conditions (Fig. 5B).

The bimetallic FeCuNR (Fig. 5C) maintained the J-aggregation structure after successive additions of H_2O_2 with an increasing absorption response of the monomer band (435 nm). This result provides further evidence of the presence of the more stable oxo-bridged Fe and Cu interaction that is slightly affected by the presence of the hydrogen peroxide. The structure of the NR remains unchanged up to 100 μM of H_2O_2.

The graph of absorbance vs. H_2O_2 concentration of the bimetallic structure (Fig. 6) reveals a sigmoid curve with an induction period in the binding of a ligand, as expected for a positive cooperativism. The moderately linear response from 15 μM to 50 μM fits to a straight line ($y = 0.00264\ \mu M^{-1}x - 0.0274$, $R^2 = 0.9797$).

We applied the Hill equation for non-hyperbolic kinetics to analyze this data (Eq. (1))

$$A = \frac{A_{max} \cdot [H_2O_2]^n}{[H_2O_2]_{0.5}^n + [H_2O_2]^n} \quad (1)$$

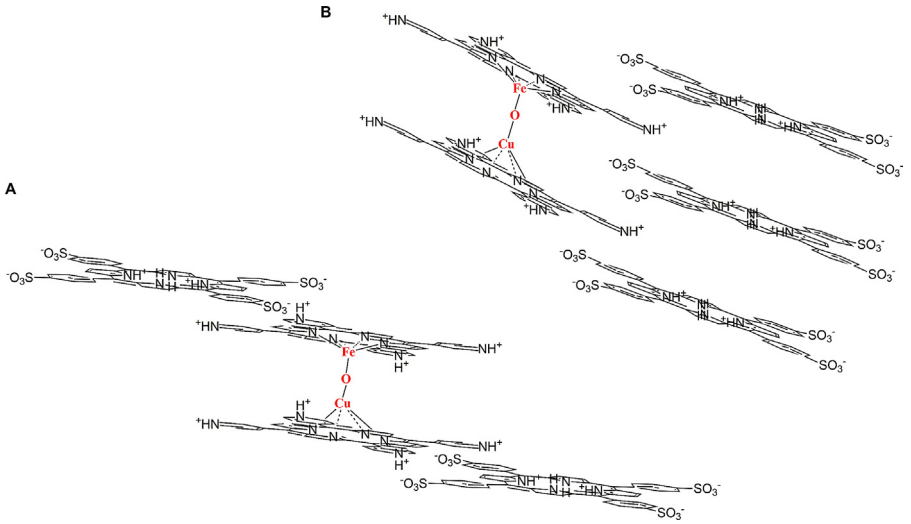

Scheme 1. Schematic representation of the proposed molecular organization.

where A is the absorbance at 435 nm, $[H_2O_2]$ is the substrate concentration (μM), $[H_2O_2]_{0.5}$ the H_2O_2 concentration necessary to coordinate the 50% of the bimetallic centers (μM), A_{max} the maximum rate and n the cooperativity index or number of Hill. The apparent Michaelis-type constant (K') is numerically equal to the substrate concentration at half-saturation.

Considering this equation, we calculate n for two different concentrations of the nanorod solutions; 180 μM ($n = 2.55$) and 60 μM ($n = 2.83$). These values reinforce the idea of a positive cooperativity between the bimetallic centers [10]. The constant rates found were $K' = 2.56 \times 10^4$ ($n = 2.83$) and $K' = 2.83 \times 10^2$ ($n = 2.55$), revealing that the more diluted solution resulted the more sensitive option.

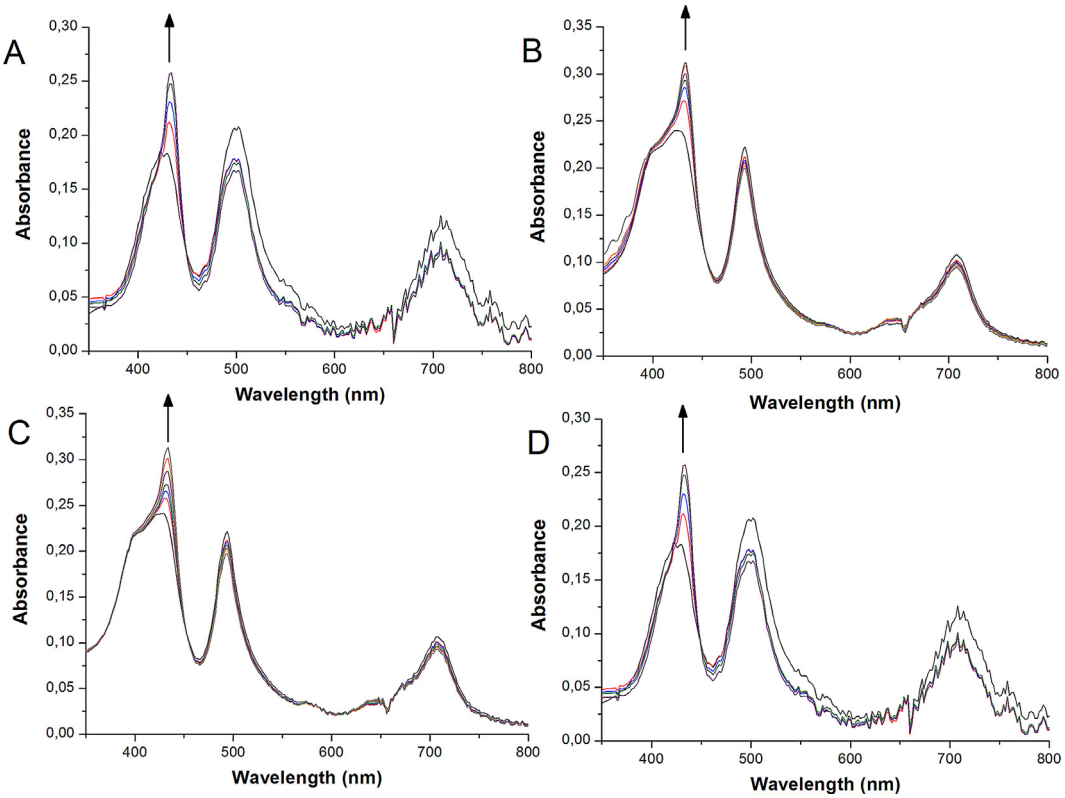

Fig. 4. Absorbance spectra of FeCuNR after successive additions of 5 μL of: (A) H_2O_2, (B) $NaNO_2$, (C) SO_3Na_2 and (D) Azide in 0.1 mol/L aqueous HCl solution. (Final concentrations: H_2O_2, 10, 20, 30, 50, 70, 80, 90 and 100 μM; $NaNO_2$, 52.5, 105, 157.5, 210, 262.5, 315 μM; SO_3Na_2, 40, 80, 120, 160, 200, 240 μM; Azide 10, 20, 30, 50, 70, 80, 90 and 100 μM).

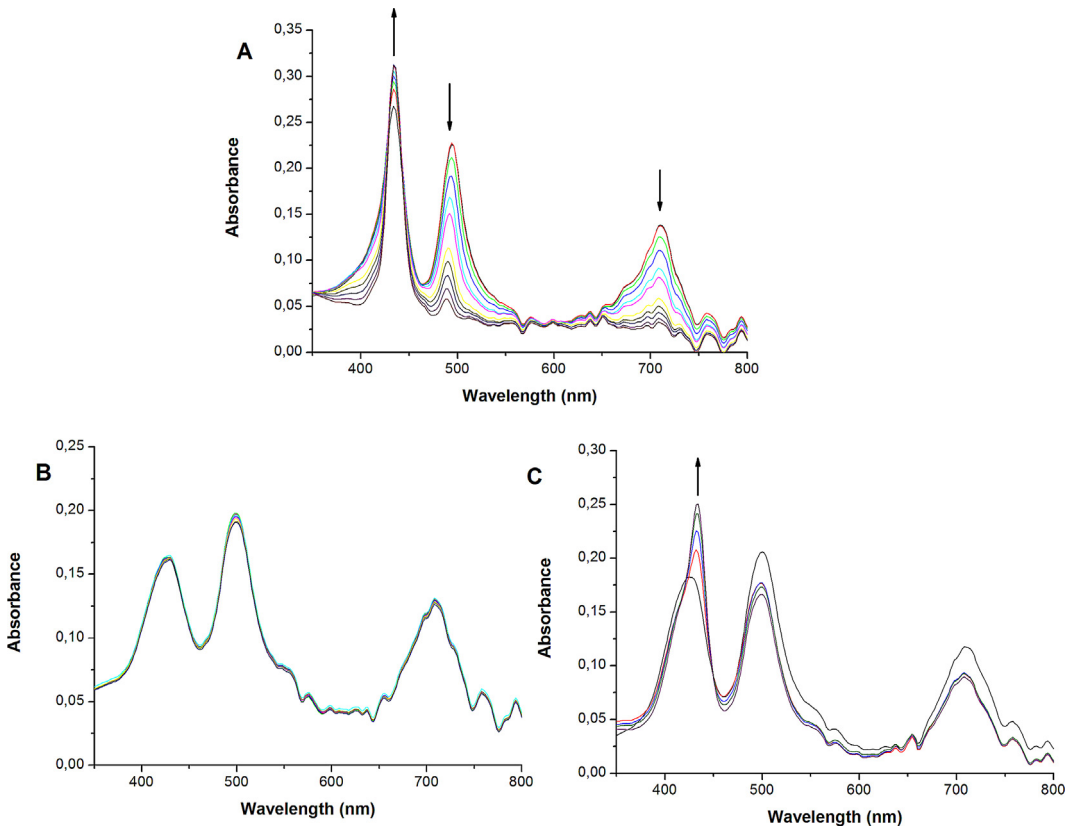

Fig. 5. Absorbance spectra of: (A) FeNR, (B) CuNR and (C) FeCuNR, after successive additions of 5 μL H_2O_2 (20 mM), in 0.1 mol/L aqueous HCl solution. (Final concentrations: 10, 20, 30, 40, 50, 60, 70, 80, 90 and 100 μM).

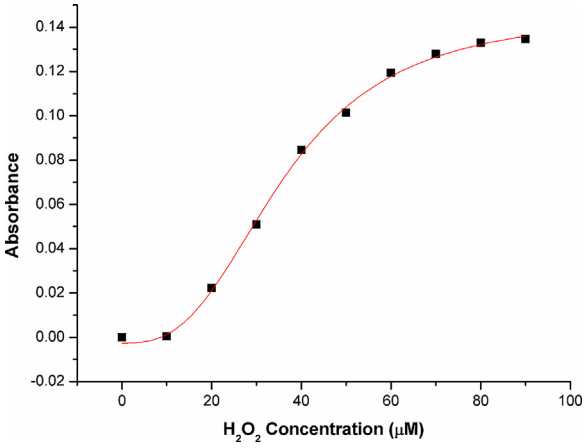

Fig. 6. Optical absorption spectroscopy vs. [H_2O_2] of FeCuNR, described by Hill equation for non-hyperbolic kinetics (Eq. (1)), $R^2 = 0.99833$.

4. Conclusions

The FeCuNR show a defined architecture related to the formation of oxo-bridged Fe and Cu cationic porphyrins. The optical response of these structures is highly sensitive to the presence of ligands. Here, we corroborate the synergic effect of the two metal complexes in a new system, where the oxo-bridged Fe and Cu interaction ($Fe^{III}OCu^{II}$) is included in a supramolecular tubular structure of porphyrins.

Acknowledgements

Financial support from University of Buenos Aires (UBACyT 0915), ANPCyT (PICT 01957) and CONICET (PIP 100076) are gratefully thanked. Mariana also thanks CONICET for her doctoral fellowship and Evelyn Hamer for the language revision.

References

[1] F.J.M. Hoeben, P. Jonkheijm, E.W. Meijer, A.P.H. Schenning, J. Chem. Rev. 105 (2005) 1491–1546 (and references therein).
[2] C.D. Dimitrakopoulos, P.R.L. Malenfant, Adv. Mater. 14 (2002) 99–117 (and references therein).
[3] T. Kobayashi (Ed.), J-Aggregates, World Scientific Publishing, Singapore, 1996.
[4] O. Ohno, Y. Kaizu, H. Kobayashi, J. Chem. Phys. 99 (1993) 4128–4132.
[5] J.-H. Chou, M.E. Kosal, H.S. Nalwa, N.A. Rakow, K.S. Suslick, Applications: past, present and future, in: K.M. Kadish, K.M. Smith, R. Guilard (Eds.), The Porphyrins Handbook, vol. 6, Acad. Press, New York, 2000, pp. 43–131 (chapter 41).
[6] C.J. Medforth, Z. Wang, K.E. Martin, Y. Song, J.L. Jacobsens, J.A. Shelnutt, Chem. Commun. 47 (2009) 7241–7428 (and references therein).
[7] Z. Wang, C.J. Medforth, J.A. Shelnutt, J. Am. Chem. Soc. 126 (2004) 15954–15955.
[8] S. Nardis, G. Pomarico, L. Tortora, R. Capuano, A. D'Amico, C. Di Natale, R. Paolesse, J. Mater. Chem. 21 (2011) 18638–18644.
[9] M. Hamer, R.R. Carballo, I.N. Rezzano, Sens. Actuators B: Chem. 160 (2011) 1282–1287.
[10] R.R. Carballo, V.C. Orto, I.N. Rezzano, J. Mol. Catal. A: Chem. 280 (2008) 156–163.
[11] J.P. Collman, R. Boulatov, Ch.J. Sunderland, Bioinorganic and bioorganic chemistry, in: K.M. Kadish, K.M. Smith, R. Guilard (Eds.), The Porphyrin Handbook, vol. 11, Academic Press, Elsevier Science, New York, 2000, p. 2 (chapter 62).
[12] R.F. Pasternack, E.J. Gibbs, J.J. Villafranca, Biochemistry 22 (1983) 2406–2414.
[13] R.C. George, G.O. Egharevba, T. Nyokong, Polyhedron 29 (2010) 1469–1474.
[14] V. Snitka, M. Rackaitis, R. Rodaite, Sens. Actuators B 109 (2005) 159–166.
[15] C. Di Natale, D. Monti, R. Paolesse, Mater. Today 13 (2010) 47–52.
[16] D.M. Chen, T.J. He, D.F. Cong, Y.H. Zhang, F.C. Liu, J. Phys. Chem. A 105 (2001) 3981–3988.

[17] R. Franco, J.L. Jacobsen, H. Wang, Z. Wang, K. Istvan, N.E. Schore, Y. Song, C.J. Medforth, J.A. Shelnutt, Phys. Chem. Chem. Phys. 12 (2010) 4072–4077.
[18] B.A. Friesen, K.R.A. Nishida, J.L. McHale, U. Mazur, J. Phys. Chem. C 113 (2009) 1709–1718.
[19] D.M. Chen, Y.H. Zhang, T.J. He, F.C. Liu, Spectrochim. Acta A 58 (2002) 2291–2297.
[20] S.G. Kruglik, P.A. Apanasevich, V.S. Chirvony, V.V. Kvach, V.A. Orlovicht, J. Phys. Chem. 99 (1995) 2978–2995.
[21] W. Jentzen, M.C. Simpson, J.D. Hobbs, X. Song, T. Ema, N.Y. Nelson, C.J. Medforth, K.M. Smith, M. Veyrat, M. Mazzanti, R. Ramasseu, J.-C. Marchon, T. Takeuchi, W.A. Goddard, J.A. Shelnutt, J. Am. Chem. Soc. 117 (1995) 11085–11097.
[22] X.-Z. Song, L. Jaquinod, W. Jentzen, D.J. Nurco, S.-L. Jia, R.G. Khoury, J.-G. Ma, C.J. Medforth, K.M. Smith, J.A. Shelnutt, Inorg. Chem. 37 (1998) 2009–2019.
[23] Ch. V. Sastri, M.J. Park, T. Ohta, T.A. Jackson, A. Stubna, M.S. Seo, J. Lee, J. Kim, T. Kitagawa, E. Münck, L. Que Jr., W. Nam, J. Am. Chem. Soc. 127 (2005) 12494–12495.
[24] (a) B.B. Wayland, L.W. Olson, J. Chem. Soc., Chem. Commun. (1973) 897–898; (b) W.R. Scheidt, M.E. Frisse, J. Am. Chem. Soc. 97 (1975) 17–21.
[25] W. Nam, M.H. Lim, S.-Y. Oh, J.H. Lee, H.J. Lee, S.K. Woo, C. Kim, W. Shin, Angew. Chem. Int. Ed. 39 (2000) 3646–3649.
[26] W.R. Scheidt, Y. Ja Lee, M.G. Finnegan, Inorg. Chem. 27 (26) (1988) 4725.
[27] C. Dallacosta, W.A. Alves, A.M. Da Costa Ferreira, E. Monzani, L. Casella, Dalton Trans. 21 (2007) 2197–2206.
[28] A. Earnshaw, Norman Greenwood, Chemistry of the Elements, 2nd ed., Butterworth–Heinemann, London, 1997.
[29] N.S. Trofimova, A.Y. Safronov, O. Ikeda, Inorg. Chem. 42 (2003) 1945–1951.

Biographies

Mariana Hamer obtained her B.Sc. in Pharmacy from the University of Buenos Aires in 2007. She is currently a Teaching Assistant at the Department of Analytical Chemistry and Physicochemical in the School of Pharmacy at the University of Buenos Aires, with Prof. Irene Rezzano as supervisor. Her research area is the design of phases with molecular recognition ability.

Juan Pablo Tomba obtained his PhD in Materials Science from National University of Mar del Plata in 1998. He was postdoctoral fellow at University of Valladolid, Spain, from 1998 to 2000, and invited Professor from 2002 to 2005 at the Chemistry Department of the University of Toronto, Canada. Currently, he is full professor at the National University of Mar del Plata and member of the Institute of Materials Science and Technology, as researcher. He is the head of the Microspectroscopy Laboratory and of the Polymer Science and Engineering Division of this Institute. His research activities focus on the characterization of polymer dynamics and structure with emphasis on microspectroscopy-based techniques.

Irene Noemí Rezzano received her B.Sc. from University of Buenos Aires in 1977 and her Ph.D. in Chemistry in 1984. From 1985 to 1988 she was a Postdoctoral Fellow in Chemistry Department at the University of California, Davis. She is currently a full professor and research leader at the Department of Analytical Chemistry and Physicochemical in the School of Pharmacy at the University of Buenos Aires. Her research interest is the design of supramolecular structures with molecular recognition ability, containing metalloporphyrins as electrochemical/optical reactive group, for sensors and biosensors applications.